# Synthesis, characterization and electrostatic properties of $WS_2$ nanostructures

Cite as: AIP Advances **4**, 057105 (2014); https://doi.org/10.1063/1.4875915
Submitted: 01 March 2014 • Accepted: 29 April 2014 • Published Online: 07 May 2014

**Yinping Fan, Guolin Hao, Siwei Luo, et al.**

AIP ADVANCES **4**, 057105 (2014)

# Synthesis, characterization and electrostatic properties of $WS_2$ nanostructures

Yinping Fan,[1,2] Guolin Hao,[1,2,a] Siwei Luo,[1,2] Xiang Qi,[1,2] Hongxing Li,[1,2] Long Ren,[1,2] and Jianxin Zhong[1,2,a]

[1]*Hunan Key Laboratory for Micro-Nano Energy Materials and Devices, Xiangtan University, Hunan 411105, P. R. China*

[2]*Laboratory for Quantum Engineering and Micro-Nano Energy Technology and Faculty of Materials and Optoelectronic Physics, Xiangtan University, Hunan 411105, P. R. China*

(Received 1 March 2014; accepted 29 April 2014; published online 7 May 2014)

We report the direct growth of atomically thin $WS_2$ nanoplates and nanofilms on the $SiO_2$/Si (300 nm) substrate by vapor phase deposition method without any catalyst. The $WS_2$ nanostructures were systematically characterized by optical microscopy, scanning electron microscopy, Raman microscopy and atomic force microscopy. We found that growth time and growth temperature play important roles in the morphology of $WS_2$ nanostructures. Moreover, by using Kelvin probe force microscopy, we found that the $WS_2$ nanoplates exhibit uniform surface and charge distributions less than 10 mV fluctuations. Our results may apply to the study of other transition metal dichalcogenides by vapor phase deposition method.  [http://dx.doi.org/10.1063/1.4875915]

## I. INTRODUCTION

The emergence of graphene has drawn much attention due to its unique properties and potential applications.[1,2] Nevertheless, the absence of graphene band gap hinders its usefulness in field effect transistors because of the low current on/off ratio. Therefore, many other layered materials, such as boron nitride,[3] and topological insulators, have been prepared and extensively studied.[4–6] Recently, layered transition metal dichalcogenides ($MX_2$ (M=Mo, W; X=S, Se) have attracted a great deal of attention for their wide applications in the field of optoelectronics,[7–10] catalysis,[11,12] energy harvesting,[8] and nano-electromechanical systems.[13]

The $WS_2$ has a layered structure of S-W-S stacking layers made up from a basic unit cell, which is held together by van der Waals forces (Figure 1(a)). Recent investigations have demonstrated that $WS_2$-based devices have high performance with low power consumption at room temperature.[14,15] The transition from indirect-to-direct band gap occurs when the dimension is reduced from bulk to monolayer, which shows promising applications in valleytronics and valley-based optoelectronics.[16] Therefore, the controllable nanostructure synthesis of these materials becomes essential. In this work, our studies are mainly focused on the synthesis and characterization of $WS_2$ nanostructures.

Currently, various methods have been employed to fabricate $WS_2$, including micromechanical cleavage technique,[16] chemical exfoliation,[17] and hydrothermal synthesis.[18] However, the thickness and size of the flakes are not controllable by these methods, which are infeasible for the integration of corresponding devices. High quality $WS_2$ nanostructure synthesis remains challenging. Chemical vapor deposition (CVD) is the most expected method to synthesize single-layer, uniform and large scale $WS_2$ films. However, previous reports indicate that large areas of $WS_2$ thin films are mainly obtained by using $WO_3$,[19–21] $HS_2$ or sulfur as the reactants.[22,23]

[a]Corresponding author. Tel.: +86 0731-58293749; fax: +86 0731-58298612. E-mail: jxzhong@xtu.edu.cn, guolinhao@xtu.edu.cn

 

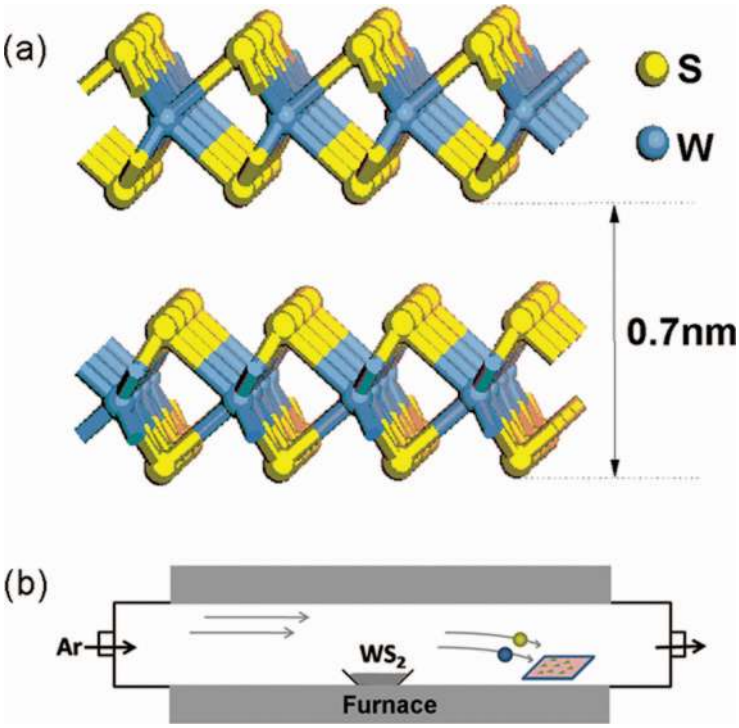


FIG. 1. (a) Lattice structure of layered $WS_2$. (b) Schematic of CVD process for the growth of $WS_2$ nanostructures.

Herein, we report a simple vapor phase deposition method for the growth of $WS_2$ nanostructures by decomposing $WS_2$ powder at high temperature. $WS_2$ nanoplates as well as a large area of thin films were directly synthesized on $SiO_2$ substrate, and were systematically characterized. The electrostatic properties of $WS_2$ nanostructures were investigated by Kelvin probe force microscopy, which has been widely applied to other layered materials such as graphene,[24] $MoS_2$ and topological insulators.[25–27] The uniform surface and charge distributions provide insight into the electronic properties of these $WS_2$ nanostructure-based devices.

## II. EXPERIMENTAL DETAILS

### A. Synthesis of $WS_2$ nanostructures

$WS_2$ nanostructures were synthesized on the $SiO_2$/Si substrate in a horizontal tube furnace (Lindberg/Blue M) by vapor phase deposition method without any catalyst as shown in the reaction setup (Figure 1(b)), which is similar to the method employed to fabricate topological insulator nanoplates in our previous reports. $WS_2$ powders (99.9%) were placed in the hot center of the furnace. The $SiO_2$/Si substrates cleaned with standard piranha solution were localized at the downstream zones 14 cm away (14-16 cm) from the hot center. The source material was heated to growth temperature (950–1000 °C) at a rate of 25 °C/min and maintained for an hour or half an hour before cooling down to room temperature naturally. During the procedure of the synthesis, the growth pressure was kept at 110 Pa within the 150 sccm Ar-$H_2$ gas flow (5% $H_2$).

### B. Characterization

The morphologies of $WS_2$ nanostructures were characterized by scanning electron microscopy (SEM, JEOL, JSM-6360) equipped with an energy dispersive X-ray spectrometer (EDX). Raman spectra were collected at room temperature in Renishaw micro-Raman spectrometer with 532 nm laser excitation light. The atomic force microscopy (AFM, SEIKO, SPI3800N + 300 HV) images

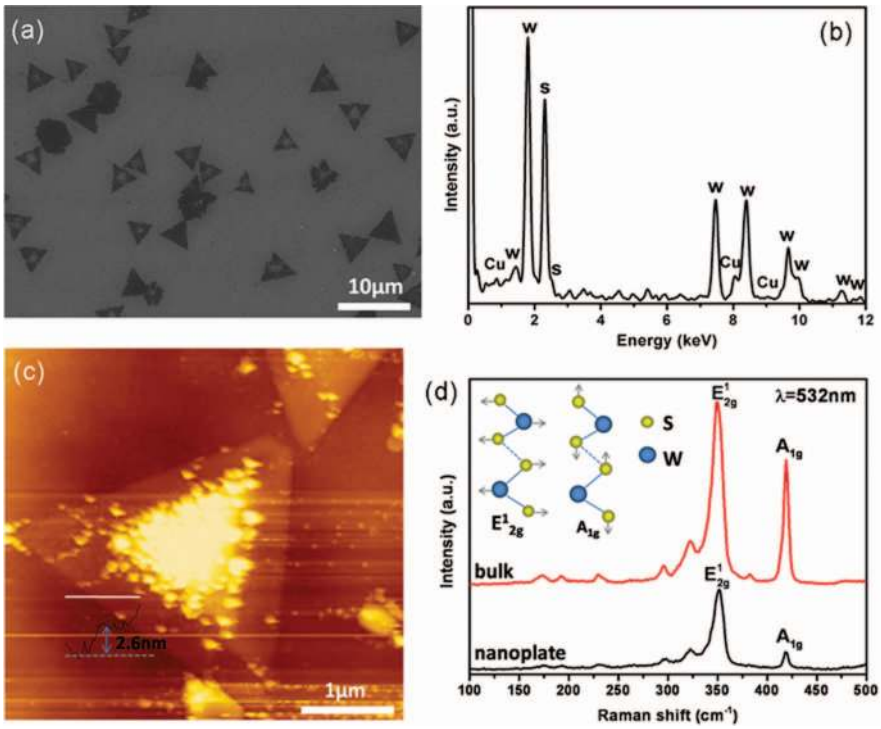


FIG. 2. (a) SEM image of triangular $WS_2$ nanoplates grown on $SiO_2$/Si subtrate. (b) EDX spectrum of synthesized $WS_2$ nanoplates. (c) AFM image of single $WS_2$ nanoplate. (d) Raman spectra of few-layer $WS_2$ nanoplates and bulk $WS_2$.

were characterized to determine the thickness of $WS_2$ nanostructures. The electrostatic properties were investigated by Kelvin probe force microscopy (AFM, SEIKO, SPI3800N + 300 HV) under ambient conditions.

## III. RESULTS AND DISCUSSIONS

Figure 2(a) exhibits a SEM image of $WS_2$ samples, which were synthesized at 1000 °C and maintained for 30 mins. It can be clearly seen that triangular $WS_2$ nanoplates were fabricated on the $SiO_2$/Si substrate with lateral dimension up to several micrometers. And the elemental compositions of synthesized $WS_2$ nanoplates were determined by EDX analysis (Figure 2(b)). The atomic contents of S and W are 66.6%, 33.4%, respectively, which are in good agreement with the $WS_2$ formula and suggests successful fabrication of $WS_2$ nanoplates.

Figure 2(c) is the AFM image of a single triangular $WS_2$ nanoplate. The thickness is ∼ 2.6 nm corresponding to 4 layers of $WS_2$, which indicates the successful synthesis of ultrathin nanoplates via vapor-solid mechanism. During the growth process, the $WS_2$ powders were heated under high temperature and decomposed to W and S atoms, which recombined at the low temperature zone. At the initial growth stage, nucleation formed randomly on the $SiO_2$/Si substate. With the formation of the nucleation centers, the incoming W and S atoms tended to bond covalently with the edge of nucleation due to the dangling bonds existence. Therefore, the growth rate of lateral dimension is fast compared to the c-axis, resulting in the formation of nanoplate structure.

Raman spectroscopy was further performed to investigate the crystal structure and quality of few-layer $WS_2$ nanoplates. For the crystal structure of $WS_2$, there are 18 lattice dynamical modes: two dominant modes of $E_{2g}$ and $A_{1g}$ are investigated in the present work. The $A_{1g}$ mode reflects the out-of-plane displacement of S atoms and the $E_{2g}$ mode involves the in-plane displacement of W and S atoms. As shown in Figure 2(d), the $E_{2g}$ and $A_{1g}$ modes of few-layer $WS_2$ nanoplates have appeared at 349.7 cm$^{-1}$ and 416.7 cm$^{-1}$, respectively. In contrast, the two modes of the $WS_2$ bulk are located at 350.3 cm$^{-1}$ ($E_{2g}$) and 418.9 cm$^{-1}$ ($A_{1g}$). $A_{1g}$ mode exhibits a blue-shift with the

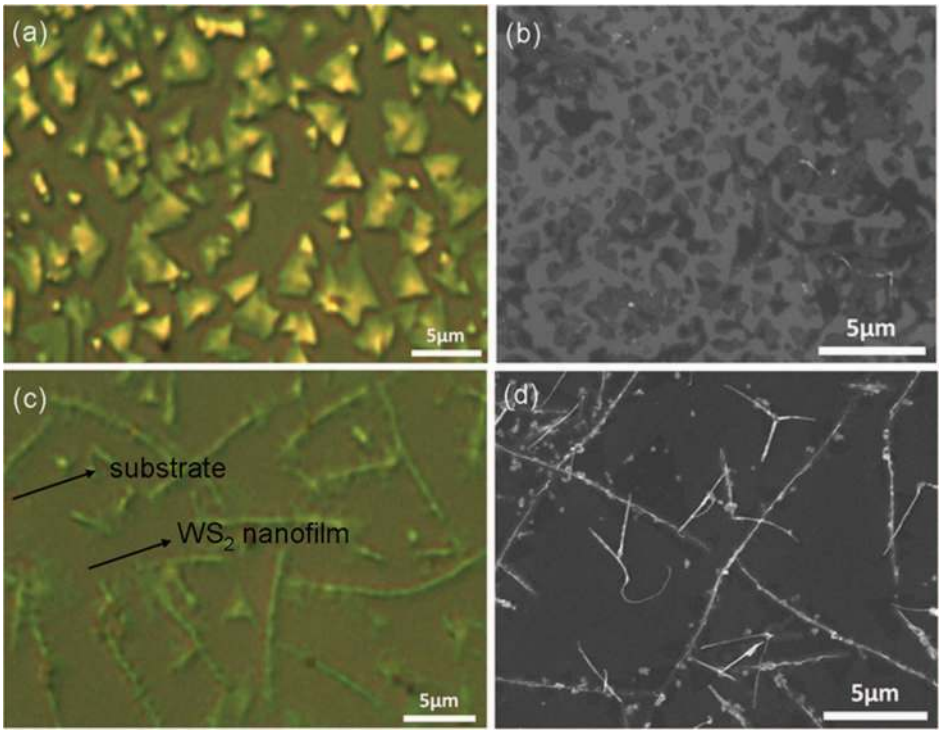


FIG. 3. (a) Photograph of few-layer $WS_2$ nanoplates on the $SiO_2$/Si substrate. (b) Corresponding SEM image. (c-d) Optical and SEM images of large area $WS_2$ films.

increase of the thickness due to the increasing van der Waals forces among layers, which is in good agreement with previous reports.[23] Our Raman results indicate high quality of synthesized $WS_2$ nanoplates.

To investigate the growth process of $WS_2$ nanostructures, the influences of growth time and temperature have been systematically conducted. When the growth time is prolonged to 60 mins under the experimental conditions mentioned above, we found that amounts of $WS_2$ nanoplates have been obtained and randomly distributed on the $SiO_2$/Si substrate. Figure 3(a) is the optical image: it clearly shows that some nanoplates merged together. The corresponding SEM image is shown in Figure 3(b). Large areas of $WS_2$ nanofilms with several hundred micrometers were simultaneously fabricated as shown in the optical and SEM images (Figure 3(c-d), which deposited on the same substrate with different distance compared with (a-b)). By comparison, we can conclude that the temperature is one of the factors, which influence the thickness and size of the $WS_2$ nanoplates. W nanowires with tens of micrometers were also obtained, which have been demonstrated by EDX analysis, further confirming the decomposition of $WS_2$ during the heating process.

It is interesting that, when the growth temperature in the hot center was reduced to 950 °C and the growth time has been maintained for 60 mins, the $WS_2$ nanoplates with random shape were synthesized (16–18 cm away from the hot center). Figure 4(a) shows the corresponding SEM image. Under such growth conditions, large areas of thin films were first grown on the whole substrate. Then the growth continues on the thin film, forming $WS_2$ nanostructures with random shapes. Figure 4(b) is a typical AFM image with the 0.5 nm surface roughness of the irregular $WS_2$ nanostructure. However, the surface roughness of the thin films is larger with 3 nm. Although the growth mechanism is not clear, the large areas of $WS_2$ nanostructure will benefit from the integration of $WS_2$-based devices.

$WS_2$ nanostructures present many promising applications in nanoelectronics and optoelectronics,[19,28] which have been extensively investigated. Nevertheless, there are few reported studies on the electrostatic properties of $WS_2$ and the interface between the $WS_2$ nanostructure and electrode, which are actually essential for the performance of $WS_2$-based devices. Herein, we

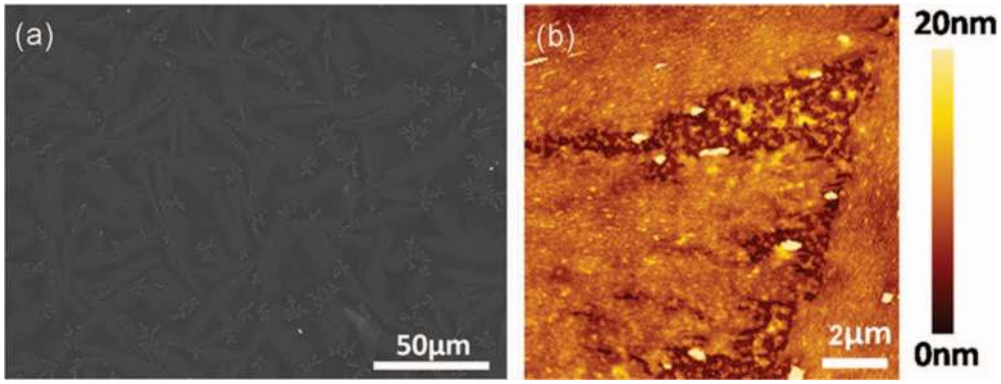


FIG. 4. (a) SEM image of irregular $WS_2$ nanofilms fabricated under 950 °C growth temperature. (b) Corresponding AFM image of $WS_2$ nanofilms.

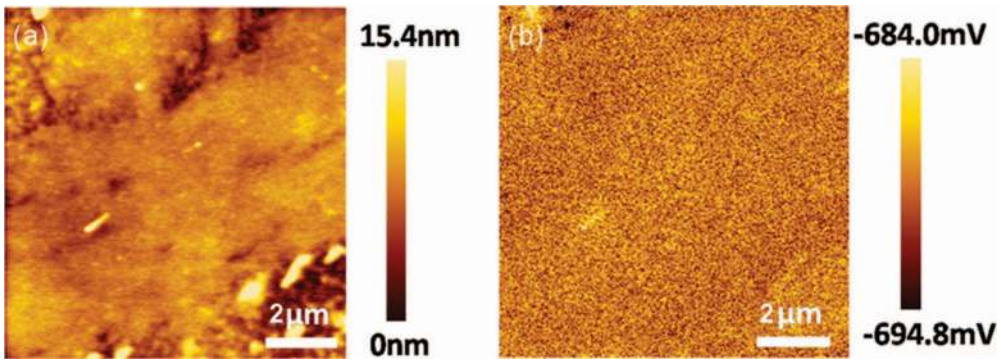


FIG. 5. (a) A typical AFM image of $WS_2$ nanofilm. (b) Corresponding surface potential image.

studied the electrostatic properties of the $WS_2$ nanostructures under ambient environment by employing Kelvin probe force microscopy. Figure 5(a) is the typical AFM image of the $WS_2$ nanostructures. Figure 5(b) is the corresponding surface potential image. The surface potential value of the $WS_2$ nanostructure is around 650 mV with 10 mV fluctuations across the whole area. The observation of the relatively homogeneous surface potential and charge distributions were observed, which also confirmed the high quality of the synthesized samples.

## IV. CONCLUSION

We have successfully fabricated the $WS_2$ nanostructures on the $SiO_2$/Si substrate via vapor phase deposition method without any catalyst. The influence of growth time and temperature on the $WS_2$ nanostructures was investigated. The results demonstrate that the temperature is one of the important factors, which influence the thickness and size of the $WS_2$ nanoplates. While, the growth time mainly affect the quantity of the samples. On the other hand, we studied the electrostatic properties of the $WS_2$ nanostructures, which exhibit a uniform surface potential and charge distributions.

## ACKNOWLEDGMENTS

This work was supported by the Grants from National Natural Science Foundation of China (Nos. 51172191, 51202208), National Basic Research Program of China (2012CB921303).

[1] K. S. Novoselov, A. K. Geim, S. V. Morozov, D. Jiang, Y. Zhang, S. V. Dubonos, I. V. Grigorieva, and A. A. Firsov, Science **306**(5696), 666–669 (2004).
[2] A. K. Geim and K. S. Novoselov, Nat. Mater. **6**(3), 183–191 (2007).

[3] J. Yu, L. Qin, Y. F. Hao, S. Y. Kuang, X. D. Bai, Y.-M. Chong, W. J. Zhang, and E. Wang, ACS Nano **4**(1), 414–422 (2010).
[4] X.-L. Qi and S.-C. Zhang, Rev. Mod. Phys. **83**(4), 1057–1110 (2011).
[5] G. L. Hao, X. Qi, Y. D. Liu, Z. Y. Huang, H. X. Li, K. Huang, J. Li, L. W. Yang, and J. X. Zhong, J. Appl. Phys. **111**(11), 114312–114315 (2012).
[6] M. Z. Hossain, S. L. Rumyantsev, K. M. F. Shahil, D. Teweldebrhan, M. Shur, and A. A. Balandin, ACS Nano **5**(4), 2657–2663 (2011).
[7] H. L. Zeng, J. F. Dai, W. Yao, D. Xiao, and X. D. Cui, Nat. Nanotechnol. **7**(8), 490–493 (2012).
[8] B. Radisavljevic, A. Radenovic, J. Brivio, V. Giacometti, and A. Kis, Nat. Nanotechnol. **6**(3), 147–150 (2011).
[9] S. F. Wu, J. S. Ross, G.-B. Liu, G. Aivazian, A. Jones, Z. Y. Fei, W. G. Zhu, D. Xiao, W. Yao, D. Cobden, and X. Xu, Nat. Phys. **9**(3), 149–153 (2013).
[10] S. F. Wu, C. M. Huang, G. Aivazian, J. S. Ross, D. H. Cobden, and X. D. Xu, ACS Nano **7**(3), 2768–2772 (2013).
[11] T. F. Jaramillo, K. P. Jørgensen, J. Bonde, J. H. Nielsen, S. Horch, and I. Chorkendorff, Science **317**(5834), 100–102 (2007).
[12] C. Choi, J. Feng, Y. Li, J. Wu, A. Zak, R. Tenne, and H. Dai, Nano Res. 1–8 (2013).
[13] A. Castellanos-Gomez, R. van Leeuwen, M. Buscema, H. S. J. van der Zant, G. A. Steele, and W. J. Venstra, Adv. Mater. **25**, 899–903 (2013).
[14] W. Sik Hwang, M. Remskar, R. Yan, V. Protasenko, K. Tahy, S. Doo Chae, P. Zhao, A. Konar, H. Xing, A. Seabaugh, and D. Jena, App. Phys. Lett. **101**(1), 013107 (2012).
[15] W. J. Zhao, R. M. Ribeiro, M. Toh, A. Carvalho, C. Kloc, A. H. Castro Neto, and G. Eda, Nano Lett. **13**(11), 5627–5634 (2013).
[16] H. Zeng, G.-B. Liu, J. Dai, Y. Yan, B. Zhu, R. He, L. Xie, S. Xu, X. Chen, W. Yao, and X. Cui, Sci. Rep. **3** (2013).
[17] H. S. S. Ramakrishna Matte, A. Gomathi, A. K. Manna, D. J. Late, R. Datta, S. K. Pati, and C. N. R. Rao, Angew. Chem. Int. Ed. **122**(24), 4153–4156 (2010).
[18] R. Huirache-Acuña, F. Paraguay-Delgado, M. A. Albiter, L. Alvarez-Contreras, E. M. Rivera-Muñoz, and G. Alonso-Núñez, J. Mater. Sci. **44**(16), 4360–4369 (2009).
[19] N. Perea-López, A. L. Elías, A. Berkdemir, A. Castro-Beltran, H. R. Gutiérrez, S. Feng, R. Lv, T. Hayashi, F. López-Urías, S. Ghosh, B. Muchharla, S. Talapatra, H. Terrones, and M. Terrones, Adv. Funct. Mater. **23**(44), 5511–5517 (2013).
[20] Y. Zhang, Y. F. Zhang, Q. Q. Ji, J. J. Ju, H. T. Yuan, J. P. Shi, T. Gao, D. L. Ma, M. X. Liu, Y. B. Chen, X. J. Song, H. Y. Hwang, Y. Cui, and Z. F. Liu, ACS Nano **7**(10), 8963–8971 (2013).
[21] Y.-H. Lee, L. L. Yu, H. Wang, W. J. Fang, X. Ling, Y. M. Shi, C.-T. Lin, J.-K. Huang, M.-T. Chang, and C.-S. Chang, Nano Lett. **13**(4), 1852–1857 (2013).
[22] S. Tiefenbacher, H. Sehnert, C. Pettenkofer, and W. Jaegermann, Surf. Sci. **318**(1–2), L1161–L1164 (1994).
[23] A. Berkdemir, H. R. Gutierrez, A. R. Botello-Mendez, N. Perea-Lopez, A. L. Elias, C.-I. Chia, B. Wang, V. H. Crespi, F. Lopez-Urias, J.-C. Charlier, H. Terrones, and M. Terrones, Sci. Rep. **3**(1755), 1–8 (2013).
[24] Z. Q. Wei, D. B. Wang, S. Kim, S.-Y. Kim, Y. K. Hu, M. K. Yakes, A. R. Laracuente, Z. T. Dai, S. R. Marder, C. Berger, W. P. King, W. A. de Heer, P. E. Sheehan, and E. Riedo, Science **328**(5984), 1373–1376 (2010).
[25] G. L. Hao, Z. Y. Huang, Y. D. Liu, X. Qi, L. Ren, X. Y. Peng, L. W. Yang, X. L. Wei, and J. X. Zhong, AIP Adv. **3**(4), 042125 (2013).
[26] Y. Li, C.-Y. Xu, and L. Zhen, Appl. Phys. Lett. **102**(14), 143110 (2013).
[27] G. L. Hao, X. Qi, L. W. Yang, Y. D. Liu, J. Li, L. Ren, F. Sun, and J. X. Zhong, AIP Adv. **2**(1), 012114 (2012).
[28] T. Georgiou, R. Jalil, B. D. Belle, L. Britnell, R. V. Gorbachev, S. V. Morozov, Y.-J. Kim, A. Gholinia, S. J. Haigh, O. Makarovsky, L. Eaves, L. A. Ponomarenko, A. K. Geim, K. S. Novoselov, and A. Mishchenko, Nat. Nanotechnol. **8**(2), 100–103 (2013).